1   **Establishment of a reverse genetic system from a bovine derived Influenza D virus isolate.**

2   Melle Holwerda [1,2,3,4], Laura Laloli [3,4], Manon Wider [3], Lutz Schönecker [2,5,6,7], Jens Becker [6,7], Mireille

3   Meylan [6,7] and Ronald Dijkman [1,2,3].

4   [1] Institute for virology and immunology, University of Bern, Bern, Switzerland.

5   [2] Department of infectious diseases and pathobiology, University of Bern, Bern, Switzerland.

6   [3] Institute for infectious diseases, University of Bern, Bern, Switzerland.

7   [4] Graduate school for cellular biology, University of Bern, Bern, Switzerland.

8   [5] Institute of Veterinary Bacteriology, Department of Infectious Diseases and Pathobiology, University

9   of Bern, Bern, Switzerland.

10   [6] Clinic for Ruminants, Vetsuisse-Faculty, University of Bern, Switzerland.

11   [7] Department of Clinical Veterinary Science, Vetsuisse-Faculty, University of Bern, Switzerland.

12

13   **Abstract**

14   The ruminant-associated Influenza D virus (IDV) has a broad host tropism and was shown to have

15   zoonotic potential. To identify and characterize molecular viral determinants influencing the host

16   spectrum of IDV, a reverse genetic system is required. For this, we first performed 5' and 3' rapid

17   amplification of cDNA ends (RACE) of all seven genomic segments, followed by assessment of the 5'

18   and 3' NCR activity prior to constructing the viral genomic segments of a contemporary Swiss bovine

19   IDV isolate (D/CN286) into the bidirectional pHW-2000 vector. The bidirectional plasmids were

20   transfected in HRT-18G cells followed by viral rescue on the same cell type. Analysis of the segment

21   specific 5' and 3' non-coding regions (NCR) highlighted that the terminal 3' end of all segments

22   harbours an Uracil instead of a Cytosine nucleotide, similar to other Influenza viruses. Subsequent

23   analysis on the functionality of the 5' and 3' NCR in a minireplicon assay revealed that these

24   sequences were functional and that the variable sequence length of the 5' and 3' NCR influences

25   reporter gene expression. Thereafter, we evaluated the replication efficiency of the reverse genetic

26   clone on conventional cell lines of human, swine and bovine origin by use of an in vitro model

27   recapitulating the natural replicate site of IDV in bovine and swine. This revealed that the reverse

28   genetic clone D/CN286 replicates efficiently in all cell culture models. Combined, these results

29   demonstrate the successful establishment of a reverse genetic system from a contemporary bovine

30   IDV isolate that can be used for future identification and characterization of viral determinants

31   influencing the broad host tropism of IDV.

32

33

34   **1. Introduction.**

35   The *Deltainfluenzavirus* genus is the newest member of the *Orthomyxoviridae* virus family,

36   and harbours the Influenza D virus (IDV) species [1,2]. In 2011, IDV was first identified in a 15-week-

37   old pig suffering from flu-like symptoms such as sneezing and dry cough [3]. Although IDV was

38   initially discovered in swine, subsequent prevalence studies proposed that cattle are the primary

39   host reservoir for IDV with a worldwide distribution [1,4–11]. In addition to cattle and swine, IDV was

40   shown to infect a broad range of other animals, such as feral swine, water buffalo, sheep, horses and

41   camelids [3,8,12–16]. Furthermore, the high seroprevalence among humans with frequent exposure

42   to cattle, as well as the recent demonstration of productive IDV replication in human airway

43   epithelial cells, indicate that the bovine-lineage of IDV has zoonotic potential [17,18].

44   Reverse genetic systems are an important tool to identify and characterize viral determinants

45   that can influence the viral host tropism [19–23]. The polarity of the segmented viral genome of

46   *Orthomyxoviruses* requires that the 6 − 8 viral genomic segments are individually transcribed in a

47   negative orientation to generate a template for the subsequent production of viral proteins and new

48   progeny virus [24,25]. The first plasmid-based reverse genetic systems for *Orthomyxoviruses* were

49   described in the late 1990s and early 2000s for Influenza A virus [26–28]. The first system consisted

50   of individual plasmids transcribing the negative sense RNA of each viral genomic segment in a RNA

51   polymerase I dependent manner [26]. These plasmids were co-transfected with eukaryotic

52   expression plasmids encoding for the nucleocapsid and RNA dependent RNA polymerase (RdRp)

53   complex proteins to initiate the production of replication competent viruses [26]. This system was

54   later modified by the more efficient bidirectional vector system that incorporates both RNA

55   polymerase I and II dependent transcription of each viral genomic segment and protein, respectively,

56   within the same backbone [27,29]. This bidirectional plasmid-based reverse genetic system has also

57   been described for Influenza B and C viruses [30,31], and more recently also for the swine lineage

58   (D/OK) of IDV [32]. Interestingly, despite cattle being the proposed main reservoir for IDV, no reverse

59   genetic system has so far been established for the more prevalent bovine-lineage [5,33,34].

60   The aim of this study is to establish a reverse genetic system for a bovine isolate of IDV,

61   which would allow for the molecular characterization of viral determinants influencing the broad

62   host tropism of IDV. For this, we first defined the 5' and 3' terminal sequences of the non-coding

63   region (NCR) of the genomic segments from a previously identified Swiss bovine IDV isolate

64   (D/bovine/Switzerland/CN286). This revealed that the first 12 and 11 nucleotides in the 5' and 3'

65   terminal NCR regions, respectively, are conserved among all the viral genome segments. However,

66   the sequence length of the NCR genomic segments influences the amplitude of the reporter gene

67   expression in a minireplicon assay. Rescue and subsequent viral replication kinetic experiments with

68   the reverse genetic clone of D/CN286 on conventional human, bovine and swine cell lines, as well as

69   well-differentiated AEC cultures from bovine and porcine origin, revealed robust viral replication.

70   These combined results demonstrate that we have established a reverse genetic system for IDV from

71   a bovine isolate that allows us for performing detailed characterization of viral determinants

72   influencing the host tropism of IDV.

73   **2. Materials and methods.**

74   **2.1 Cell culture.**

75   The Madin Darby Bovine Kidney (MDBK) cell line was maintained in Eagle's minimum

76   essential medium (EMEM; (Gibco, Gaithersburg, MD, USA) supplemented with 7% heat-inactivated

77   fetal bovine serum (FBS, Gibco), 2 mmol/L Glutamax (Gibco), 100 µg/mL streptomycin and 100 IU/mL

78   penicillin (Gibco). Human rectal tumour 18G (HRT-18G, American Type Culture Collection, Manassas,

79   VA, USA (ATCC)), Swine testicular (ST, ATCC) cells and human embryonal kidney (HEK) 293-LTV (LTV-

80   100; Cellbiolabs, San Diego, CA, USA) cell lines were maintained in Dulbecco's minimum essential

81   medium (DMEM; Gibco) supplemented with 5% (HRT-18G) or 10% (ST and 293T-LTV) FBS, 100 µg/mL

82   streptomycin and 100 IU/mL penicillin (Gibco). Well-differentiated airway epithelial cell cultures of

83   bovine and swine origin were established from post-mortem tracheobronchial epithelial tissue and

84   maintained according to the protocol by Gultom *et al.* (2020) [35]. All cell cultures were maintained

85   at 37 °C in a humidified incubator with 5% CO_2.

86   **2.2 Determination of the 5' and 3' NCRs by Rapid amplification of cDNA ends (RACE).**

87   The nucleotide sequences of the 5' and 3' NCRs of the D/bovine/Switzerland/CN286

88   (D/CN286) virus isolate were determined by an in-house protocol, based on the 5' and 3' RACE kit

89   (2nd generation, Roche, Basel, Switzerland). Viral nucleic acids were extracted from 140 µl of the virus

90   transport medium derived from the nasopharyngeal swab using the viral RNA isolation kit according

91   to the manufacturer's protocol (Qiagen, Venlo, The Netherlands). For the 3' RACE, isolated viral RNA

92   was poly-adenylated using *E. coli* poly-A polymerase (New England Biolabs, NEB, Ipswich, MA, USA)

93   for 30 minutes at 37 °C, followed by a reverse transcriptase (RT)-step with Moloney Murine Leukemia

94   Virus RT (MMLV-RT, Promega, Madison, WI, USA) in the presence of RNase inhibitor (RNAsin plus,

95   10U, Promega) by incubation for 1 hour at 42 °C and 20 minutes of 65 °C using the tagRACE_dT16

96   oligonucleotide. For 5' RACE, instead of the tagRACE_dT16 oligonucleotide, a segment-specific

97   reverse oligonucleotide was used as described above, followed by nucleic acid purification and poly-

98   adenylation of the cDNA with terminal transferase (NEB) for 30 minutes at 37 °C followed by 10

99   minutes heat-inactivation at 70 °C. For both the 3' and 5' RACE, an initial touchdown PCR was

100   performed with Hotstart Taq mastermix (Qiagen) with segment-specific primers and tagRACE_dT16

101   reverse oligonucleotides **(Supplementary Table 1)**, using the following cycle profile; 95℃ for

102   15 min; 15 cycles of 94℃ for 30 s, 65℃ touchdown to 50℃ for 1 min, 72℃ for 1 min; 25 cycles of

103   94℃ for 30 s, 50℃ for 1 min, 72℃ for 1 min. After the first amplification round, the segment-

104   specific PCR products were 100-fold diluted in nuclease free water and used as template in a nested

105   PCR using segment-specific oligonucleotides, in combination with the tagRACE adapter

106   oligonucleotide, using the touchdown PCR protocol **(Supplementary Table 1)**. Thereafter, PCR

107   products were purified using the Nucleospin Gel and PCR clean-up kit (Macherey-Nagel, Oensingen,

108   Switzerland) from which the nucleotide sequence was determined using Sanger sequencing

109   (Microsynth, Balgach, Switzerland). Sequence analysis was performed in Geneious Prime (Biomatters,

110   Auckland, New Zealand, v2020.2.4). The PB2 (5'), HEF (5'), and NS1 (3') sequences were determined

111   from purified product cloned into the pGEM-T vector by TA-cloning (Promega) according to the

112   manufacturer`s guidelines.

113   **2.3 Plasmid construction.**

114   *2.3.1 Minireplicon reporter constructs.*

115   For the generation of minireplicon reporter constructs for each of the seven genomic

116   segments of IDV, the coding sequence of the Gaussia luciferase reporter was amplified from the

117   pMCS-Gaussia (Thermo Fischer Scientific, Darmstadt, Germany) plasmid using a specific primer set

118   **(Supplementary Table 1)**, and CloneAmp HiFi PCR (Takara, Tokyo, Japan) according to

119   manufacturer`s guidelines, using the following cycle profile; 98 °C 10 seconds, 55 °C 10 seconds, 72 °C

120   10 seconds for 35 cycles. Followed by subcloning the PCR amplicon in Bam-HI (NEB) restriction

121   digested pCW57-tGFP-2A-MCS plasmid, kindly provided by Prof. Dr. Adam Karpf (Addgene plasmid

122   #71783, [36]), using the In-Fusion HD cloning kit (Takara). From the resulting pCW57-GFP-2A-Gaussia

123   plasmid, the tGFP-2A-Gaussia luciferase coding sequence was amplified using oligonucleotides

124   harbouring segment-specific NCR nucleotide sequence overhangs from the IDV D/660 isolate

125   **(Supplementary Table 1)**. The resulting seven different amplicons were individually subcloned into

126   the pHH21 vector, kindly provided by Prof. Dr. Georg Kochs, University of Freiburg, Germany, using

127   the In-Fusion HD cloning kit (Takara). As a transfection control for the minireplicon assay, the tRFP-2A

128   coding sequence was amplified from the pCW57-tRFP-2A-MCS plasmid, kindly provided by Prof. Dr.

129   Adam Karpf (Addgene plasmid #78933, [36]) **(Supplementary Table 1)**, using CloneAmp HiFi PCR

130   (Takara) and was subcloned in the Thymidine kinase Cypridina plasmid (Thermofisher) in-frame with

131   the Cypridina luciferase gene, using the In-Fusion HD cloning kit (Takara), resulting in the pTK-RFP-

132   2A-Cypridina luciferase plasmid. The polymerase complex subunits PB2, PB1, P3 and NP from D/660

133   and D/CN286 were amplified from the respective bidirectional pHW2000 plasmid constructs using

134   CloneAmp Hifi PCR mix (Takara) with the following cycle profile; 98 °C 10 seconds, 55 °C 10 seconds,

135 72 °C 20 seconds for 35 cycles followed by subcloning into the eukaryotic expression vector pCAGGs

136 using the In-Fusion HD cloning kit (Takara). All plasmids were midiprepped using the Nucleobond Xtra

137 midi kit (Macherey-Nagel), and verified by Sanger sequencing (Microsynth).

138 *2.3.2 Construction of reverse genetic clone.*

139 Two microliters of extracted viral RNA were used as template to amplify the seven genomic

140 segments individually with segment-specific oligonucleotides using the Superscript IV one-step RT-

141 PCR system (Thermo Fisher Scientific), according to manufacturer guidelines. The bidirectional

142 pHW2000-vector, kindly provided by Prof. Dr. Martin Schwemmle, University of Freiburg, Germany,

143 was amplified using CloneAmp HiFi PCR mix (Takara) in a 2-step PCR-program of 98°C for 10 seconds

144 followed by 68°C for 4 minutes, with 35 cycles. Both PCR products were excised from a 1% agarose

145 gel and extracted using the Nucleospin Gel and PCR clean-up kit (Macherey-Nagel) and used as

146 templates for In-Fusion HD cloning (Takara). Positive constructs were identified by colony PCR using

147 the segment-specific PCR primers and Taq green mastermix (Promega) with the following cycle

148 profile; 94°C 5 minutes, followed by 25 cycles of 94°C, 1 minute, 55°C 1 minute, 72°C 2 minutes, and

149 a final elongation step of 7 minutes at 72°C. All plasmids were midiprepped using the Nucleobond

150 Xtra midi kit (Macherey-Nagel), and verified by Sanger sequencing (Microsynth).

151 **2.4 Minireplicon assay.**

152 One day prior to the minireplicon assay, 293-LTV cells were seeded at a density of 25.000

153 cells per well, in black-wall, clear bottom 96-well plates (Costar, Corning, NY, USA) in DMEM medium

154 containing 15 mM HEPES (Gibco). For each minireplicon reaction, 50 ng of reporter plasmid

155 containing one of the IDV segment specific NCR was mixed with 100 ng of each polymerase subunit

156 (PB2, PB1 and P3) and 200 ng of NP in the eukaryotic expression vector pCAGGs in 50 µl of Optimem

157 (Gibco), together with 250 ng of pTK-RFP-2A-Cypridina luciferase as transfection control. An equal

158 amount of Optimem containing PEImax (1 mg/ml, Polysciences, Warrington, PA, USA) in a 1:3

159 DNA:transfection reagent ratio was prepared and added to the overexpression plasmids. After 20

160 minutes of incubation at room temperature, 20 µl volumes from the transfection mixture were

161 divided into three technical replicates. The polymerase activity based on secreted luciferase activity

162 was monitored, by collecting 50 µl of supernatant and replenishment with fresh medium every 24

163 hours. Supernatant samples were stored at -80°C for subsequent analysis. In parallel, the polymerase

164 activity was monitored by the detection of fluorescence reporter expression on a Cytation 5 Cell

165 Imaging Multi-Mode Reader (BioTek, Sursee, Switzerland) equipped with a 4x air objective

166 (numerical aperture (NA): 0.13). Four images per well were acquired to cover the entire surface of

167 the well and processed and stitched using the Gen5 Image prime software package (v3.08.01). The

168   number of cells that express turbo green fluorescent protein (tGFP, polymerase activity) or turbo red
169   fluorescent protein (tRFP, transfection control) were determined for each individual well using the
170   Gen5 ImagePrime software package (v3.08.01). Gaussia and Cypridina luciferase activities were
171   measured separately in the collected supernatant samples using the Pierce Gaussia or Cypridina
172   luciferase flash assay kits (Thermo Fischer Scientific), respectively, on a Cytation 5 Cell Imaging Multi-
173   Mode Reader (BioTek). Ten µl of supernatant per reaction were loaded into white, half area 96-well
174   plates (Costar), followed by the injection of 15 µl of substrate and direct measurement of the
175   luminescent signal.

176   **2.5 Rescue of IDV from reverse genetic plasmids.**

177   One day prior to virus rescue, 1 million HRT-18G cells per well were seeded into 6-well plates
178   (Techno Plastic Products AG (TPP), Trasadingen, Switzerland). For every viral rescue, each viral
179   segment in the bidirectional pHW2000 plasmid was diluted to a concentration of 0.2 µg per reaction,
180   followed by transfection using PEImax (1 mg/ml) in a 1:3 DNA:transfection reagent ratio. After 48
181   hours of incubation at 37°C in a humidified incubator with 5% CO_2, the supernatant was removed,
182   and cells were washed twice with MEM medium. After the final washing, cells were supplemented
183   with infection medium, consisting of MEM with 0.5% bovine serum albumin (Sigma-Aldrich), 15 mM
184   of HEPES (Gibco), 100 µg/ml of penicillin and 100 IU of streptomycin (Gibco), and 0,25 µg/ml of
185   bovine-pancreas isolated trypsin (Sigma-Aldrich). Thereafter, cells were incubated for an additional
186   72 hours at 37°C. Hereafter, the collected supernatant was diluted 10-fold and inoculated onto a
187   confluent layer of HRT-18G cells seeded in a 6-well cluster plate and incubated for 72 hours at 37°C in
188   a humidified incubator with 5% CO_2. The final virus stock was collected and titrated by tissue culture
189   infectious dosis 50 ($TCID_{50}$) method, as described previously [18]. Rescued viruses were sequence-
190   verified with Sanger sequencing through the amplification of individual genomic segments, as
191   described above.

192   **2.6 Nucleotide homology analysis.**

193   Nucleotide sequences of each segment of the prototypic D/bovine/Oklahoma/660/2013
194   (D/660, accession numbers: KF425659-65) were analysed for their homology to the D/CN286
195   consensus sequences determined by MINion Nanopore sequencing (Glaus *et al.*, Manuscript in
196   preparation) in Geneious prime (v2020.2.4).

197   **2.7 Viral replication kinetics.**

198   One day prior to infection, the conventional cell lines HRT-18G and ST were seeded at a
199   density of 250.000 cells per well in a 12-well format (TPP), while 125.000 cells were used for the

200   MDBK cell line. Viral infection was performed as previously described, using an MOI of 0.01 for the
201   HRT-18G and ST cell lines, while the MDBK cell line was infected with an MOI of 0.1 [18]. The well-
202   differentiated AEC cultures of porcine and bovine origin were inoculated with 10.000 TCID$_{50}$ per
203   insert. For the conventional cell lines, the viral replication kinetics were monitored for 72 hours in 24-
204   hour intervals, at which 250 µl of supernatant was collected and replenished with fresh medium.
205   While progeny virus production was monitored for 96 hours for the well-differentiated porcine and
206   bovine AEC cultures, the apical wash was collected every 24 hours as described before [18]. After the
207   last time point, cells were fixed with 4% *(V/V)* neutral buffered formalin and prepared for
208   immunostaining (Formafix AG, Hittnau, Switzerland).

209   **2.8 Immunostaining.**

210   Formalin-fixed conventional cell cultures and well-differentiated AEC cultures were
211   immunostained according to a previously described protocol [35]. For the detection of IDV-positive
212   cells, cell cultures were stained with a custom-generated rabbit polyclonal antibody directed against
213   the NP of the prototypic D/bovine/Oklahoma/660/2013 strain (Genscript, Piscataway, NJ, USA) [18].
214   Alexa Fluor®488-labeled donkey anti-Rabbit IgG (H+L) (Jackson Immunoresearch) was applied as
215   secondary antibody. For the porcine and bovine AEC cultures cilia and tight junctions were visualized
216   using an Alexa Fluor® 647-conjugated rabbit anti-β-tubulin IV (9F3, Cell Signaling Technology,
217   Danvers, MA, USA) and Alexa Fluor® 594-conjugated mouse anti-ZO-1 (1A12, Thermo Fisher
218   Scientific). All samples were counterstained using 4',6-diamidino-2-phenylindole (DAPI, Thermo
219   Fisher Scientific) to visualize nuclei. Images for the HRT-18G, ST, and MDBK cell lines were acquired
220   on the EVOS FL auto 2 fluorescence microscopes (Thermo Fischer Scientific), using a 10x air (NA: 0.3)
221   objective. For the AEC cultures, inserts were mounted on Colorforst Plus microscopy slides (Thermo
222   Fisher Scientific) in Prolong diamond antifade mountant (Thermo Fisher Scientific) and overlaid with
223   0.17 mm high precision coverslips (Marienfeld, Lauda-Königshofen, Germany). Z-stack images were
224   acquired on a DeltaVision Elite High-Resolution imaging system (GE Healthcare Life Sciences, Chicago,
225   IL, USA) using a step size of 0.2 µm with a 60×/1.42 oil objective. Acquired images were cropped and
226   deconvolved using the integrated softWoRx software package and processed using Imaris (Version
227   9.4.3, Bitplane AG, Zürich, Switzerland) and FIJI [37].

228   **2.9 Data representation.**

229   All graphs were generated using GraphPad Prism software (Prism, San Diego, CA, USA, v9.0.0)
230   and final figures were assembled in Adobe Illustrator CS6 (v16.0.0). Brightness and contrast of
231   microscopy picture were minimally adjusted and processed identically to their corresponding control
232   using FIJI (v1.53) [37].

233   **3. Results.**

234   **3.1 Determination of the 5' and 3' NCRs of the genomic segments from a bovine IDV isolate.**

235   IDV has been shown to infect a broad range of animal species including cattle, swine and
236   small ruminants, with cattle as the proposed main host reservoir [1]. However, so far no reverse
237   genetic system has been established for a bovine isolate of IDV, that can be used to characterize viral
238   determinants which influences the broad host tropism of IDV among even-toed ungulates. We
239   previously determined the prevalence of IDV in a Swiss cattle cohort and analysed the phylogenetic
240   relationship of 10 clinical isolates to that of other IDV isolates (Glaus *et al.*, Manuscript in
241   preparation). During this study we did not determine the 5' and 3' NCRs of each genomic segment.
242   However, because of the importance of the NCR in viral replication and the previous reported
243   sequence discrepancy among different IDV isolates in public sequence repositories, we decided to
244   determine the 5' and 3' NCR sequences of the genomic segments from one of our bovine IDV isolates
245   [38]. Based on the Ct-value and available amount of nasopharyngeal material, this was chosen to be
246   the D/Switzerland/bovine/CN286 isolate (Glaus *et al.*, Manuscript in preparation).

247   We first performed 3' RACE for each genomic segment and readily observed that all seven
248   genomic segments have a terminal Uracil nucleotide at the 3' end of the genome, similar to other
249   Influenza viruses, and found that the first 11 nucleotides (UCGUAUUCGUC) of the 3' NCR are
250   conserved among all genomic segments **(Figure 1)** [39–42]. This finding corroborates the previous
251   results from Ishida and colleagues (2020) and independently highlighted that the terminal nucleotide
252   of the 3' NCR of genomic segments from several isolates are incorrectly annotated in public sequence
253   repositories, including the prototypic D/Oklahoma/Bovine/660 isolate [38]. The results from the 5'
254   RACE revealed that the first 12 nucleotides are uniform for all seven genomic segments
255   (AGCAGUAGCAAG) and correspond with the public available sequence data for IDV **(Figure 1)**. In line
256   with this observation, the constant terminal universal motif in the 5' and 3' NCR in our bovine IDV
257   isolate is followed by a segment-specific variable sequence region that seems to be conserved among
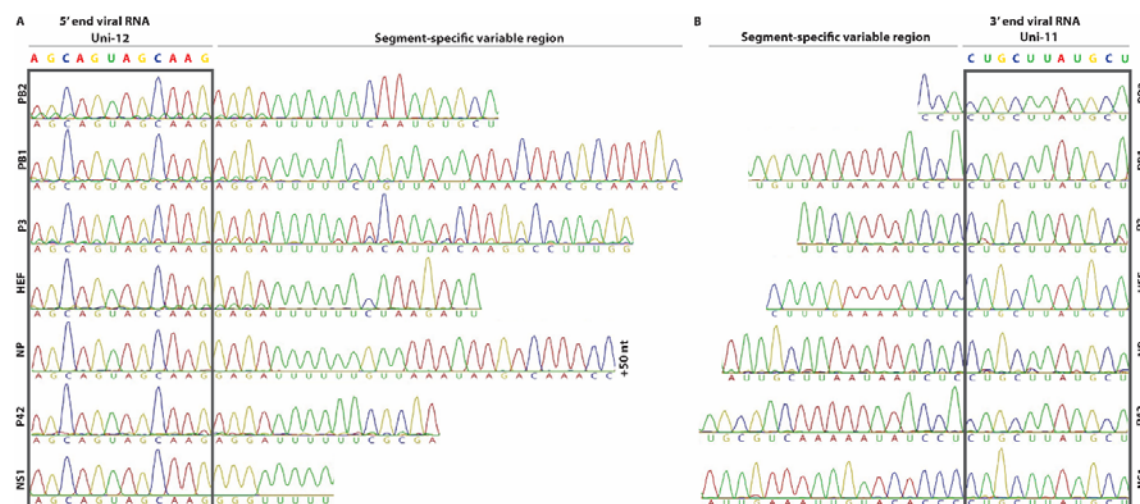258   different IDV isolates **(Figure 1)**.

259

Figure 1: 5' and 3' RACE sequence results of the non-coding regions from the D/bovine/Switzerland/CN286 virus isolate. The 5' and 3' non-coding regions were determined via Sanger sequencing of 5' and 3' rapid amplification of cDNA ends (RACE) PCR amplified products. The conserved first 11 nucleotides (UCGUAUUCGUC) and the first 12 nucleotides (AGCAGUAGCAAG) of the 3' and 5' NCR, respectively, of the viral RNA are highlighted and adjacent to the segment-specific variable regions.

3.2 Analysis of the functionality of the different NCRs by polymerase reconstitution assay.

Following the sequence determination of the 5' and 3' NCR for each of the seven genomic segments, we wanted to investigate whether the segment-specific NCRs of IDV are functional and whether the nucleotide sequence length influences the transcription and replication efficiency of viral genomic segments. Traditionally, these assays are performed with a plasmid-driven polymerase reconstitution assay (minireplicon). This assay is based on the transfection of eukaryotic expression constructs encoding for the PB2, PB1 and PA/P3 polymerase subunits and the nucleoprotein (NP) in-trans with a plasmid that transcribes a negative strand RNA harbouring a reporter gene (e.g. firefly luciferase) that is flanked by the 3' and 5' NCR regions of a viral genomic segment [43,44]. This type of assay is often limited to one timepoint due to the readout method requiring lysis of the transfected cells. To overcome this, we established a reporter construct for IDV that harbours a tGFP-2A-Gaussia luciferase reporter, which allowed us to monitor and measure the influence of the NCR sequence length on gene expression at multiple time points simultaneously via fluorescent- and luciferase-based quantification assays **(Figure 2A)**. To control for the transfection efficiency, we established a control plasmid that constitutively expresses a tRFP-2A-Cypridina luciferase and can be used in parallel for the normalization of the expression of both the tGFP and Gaussia luciferase reporter genes **(Figure 2A)**.

To demonstrate the functionality of this minireplicon assay, we first monitored the activity of the viral RNP complex of the prototypic D/660 isolates, as this virus replicates in cell cultures. This

285   revealed that the tRFP fluorescent signal could be readily observed 24 hours post-transfection, and

286   that a large number of tGFP positive cells were detected in those cells containing the reporter

287   construct with the NCR of the NP viral genomic segment after 72 hours **(Figure 2B)**. Here we

288   observed that the highest reporter activity is detected for the NCR of the NP viral genomic segment

289   followed by those for PB1, PB2, P3 and P42 **(Figure 2C)** with equal transfection efficiencies **(Figure**

290   **2D)**. In contrast, the reporter activity for NS remained relatively low and the fluorescent signal of the

291   HEF NCR was undetectable, similar to the control cells that lacked a reporter plasmid **(Figure 2C)**.

292   These results were corroborated when we analysed the activity of the D/CN286 RNP complex.

293   Despite the fact that several amino acid differ between the D/CN286 and D/660 RNP complex

294   subunits, a relatively similar activity was demonstrated, albeit with a moderately higher activity for

295   the latter **(Figure 2E, F, Supplementary Table 2)**. The results obtained with the fluorescent-based

296   assay were corroborated by the luciferase-based assay **(Figure 2G, H)**. Interestingly, this revealed

297   that the reporter activity of NS is approximately 10-100-fold lower compared to that of NP, PB1, PB2,

298   PA, and P42, while for HEF this is even lower **(Figure 2G, H)**. Because we previously observed that

299   temperature potentially influences the replication kinetics of IDV [18], we also assessed the RNP

300   complex activity with the different NCR reporter constructs at 33°C. We observed that the

301   transfection efficiencies and the number of tGFP positive cells for both the D/660 and D/CN286 RNPs

302   are identical at 33°C in comparison to 37°C **(Supplementary Figure 1)**. However, based on the

303   luciferase activity, we observed that the reporter activity as well as fluorescence intensity were lower

304   at 33°C in comparison to 37°C. This minireplicon assay readout is likely influenced by the

305   temperature dependence of protein folding kinetics **(Supplementary Figure 1)** [45]. Nonetheless,

306   these combined results clearly demonstrate that the NCR of the different constructs are active and

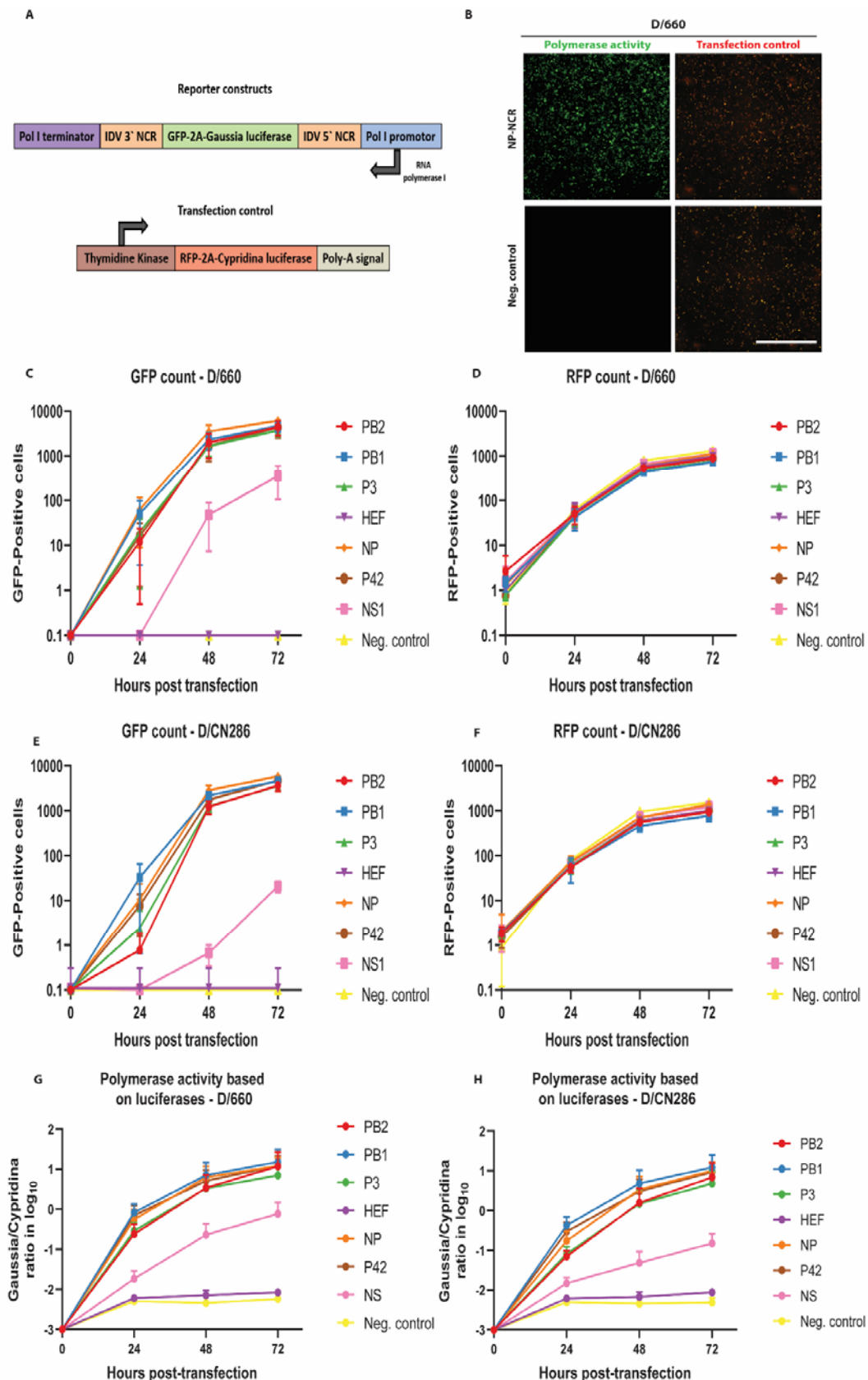307   that the nucleotide sequence length influences the transcription efficiency of the viral genomic

308   segments.

309

310   **Figure 2: Analysis of the functionality of each segment-specific non-coding region (NCR) of**
311   **Influenza D virus (IDV) by polymerase reconstitution assay (minireplicon).** 293-LTV cells were
312   transfected with expression plasmids encoding for the ribonucleoprotein (RNP) polymerase subunits
313   PB2, PB1, P3 and NP of the D/bovine/Oklahoma/660/2013 (D/660) or D/bovine/Switzerland/CN286
314   (D/CN286) virus isolates, together with a reporter and transfection control. **(A)** Illustration of the
315   reporter and transfection plasmids, whereby the tGFP-2A-Gaussia luciferase coding sequence in the
316   reporter plasmid is flanked by the 5` and 3` NCR of one specific viral genomic segment. The
317   transfection control plasmid expresses the tRFP-2A-Cypridina luciferase polyprotein under control of
318   the Herpes Simplex virus Thymidine Kinase (TK) promoter. The RNP complex activity was monitored
319   for 72 hours by acquiring images and collecting supernatant samples every 24 hours. **(B)**
320   Representative microscopy images of the D/660 virus RNP complex activity (green) with the NP NCR
321   reporter and transfection control (red) at 72 hours post transfection. Images are representative of
322   three individual experiments performed in three technical replicates. Scale bar is 2000 µm. The
323   counted GFP **(C, E)** and RFP **(D, F)** positive cells of the respective D/660 **(C, D)** and D/CN286 **(E, F)** RNP
324   complexes. Normalized RNP activity of the D/660 **(G)** and D/CN286 **(H)** based on secreted luciferases.
325   Results are displayed as means and SD of three individual experiments performed in three technical
326   replicates.

327   **3.3 Establishing a reverse genetic system for IDV.**

328   After establishing the functionality of the NCR regions, the individual viral genomic segments
329   from both the bovine D/660 and D/CN286 isolates were cloned into the bidirectional pHW2000-
330   vector for the rescue of a reverse genetic clone of a bovine IDV isolate **(Figure 3A, B)** [27].
331   Sequencing of the obtained pHW2000 plasmids revealed that there were three amino acids between
332   the D/CN286 genetic clone and the consensus sequence from the clinical isolate, namely in the PB1
333   (D388N), P3 (R350K) and HEF (Q48P). While the plasmids from the D/660 genetic clone were
334   identical to the previous published sequences, except for the terminal Uracil nucleotides in the 3'
335   NCR.

336   Following cloning, we transfected the reverse genetic plasmids for rescue of our D/660 and
337   D/CN286 clones into HRT-18G cells, as these cells support the propagation of IDV. After 72 hours of
338   incubation, the supernatant from the transfected cell cultures was collected and passaged upon fresh
339   cultures of HRT-18G followed by viral titration. During the transfection and subsequent passage, we
340   observed no cytopathogenic effect, which was also observed for the cell culture isolate of D/660
341   (data not shown). However, during the viral titration, that was based on the readout of the
342   agglutination of chicken red blood cells, we measured rescued virus with a viral titre of
343   approximately 10^7 Tissue culture infectious dose (TCID$_{50}$) per millilitre for the D/CN286 rescued virus,
344   while surprisingly no virus was detected for the D/660 reverse genetic clone **(Figure 3C)**. Whole
345   genome sequencing of the passage 1 of the rescued D/CN286 clone revealed that the sequence was
346   identical to that of the reverse genetic plasmids, whereas for D/660 this could not be established.

347
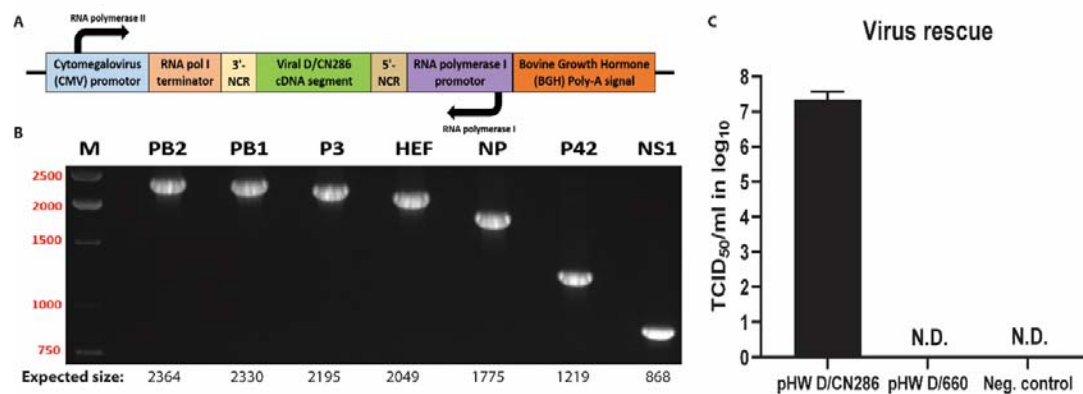
Figure 3: Establishment of a reverse genetic system for IDV. (A) A schematic representation of the genetic elements present in the bidirectional pHW2000-backbone. **(B)** PCR confirmation of cloning the individual viral genomic segments into the pHW2000 plasmid using segment-specific primers. The PCR products were analysed by gel electrophoresis analysis on a 1% agarose gel. The expected fragment sizes are annotated under each lane for each viral genomic segment. **(C)** Viral titres of the reverse genetic clones D/CN286, D/660, and the negative control after a single passage on HRT-18G-cells. Results are shown as means and SD of three individual experiments performed in two technical replicates per condition. **Abbreviations:** N.D.: not detected.

In the absence of a reverse genetic clone for D/660 and the retrospective identification of another respiratory virus, namely bovine coronavirus, in the CN286 clinical sample, we could not compare the replication kinetics of our rescued D/CN286 reverse genetic clone to the parental strain. Therefore, we instead compared the replication kinetics of the D/CN286 reverse genetic virus with that of the prototypic D/660 cell culture isolate on different cell culture models. We first monitored the viral kinetics on swine (ST), bovine (MDBK) and human (HRT-18G) cell lines for a total duration of 72 hours. This revealed that the replication kinetics of the reverse genetic D/CN286 clone on HRT-18G and ST cell lines is comparable to the cell culture isolate of D/660 **(Figure 4A, B)**. In contrast, the replication kinetics of D/CN286 on the bovine MDBK cell line was approximately 10-fold less efficient compared to the cell culture-adapted D/660 isolate **(Figure 4C)**. In addition to the replication kinetics, we performed immunostaining using a polyclonal NP-directed antibody [18]. This demonstrated that a comparable amount of virus-antigen positive cells could be detected despite the differences in the replication kinetics between both viruses **(Figure 4D-F)**.

Because the reverse genetic D/CN286 isolate was shown to efficiently replicate in cell lines derived from different species, and we aim to characterize viral determinants that can influence the viral host tropism of IDV, we wondered whether this virus would also infect *in vitro* cultures that recapitulate the natural target site of IDV. To this extend, we inoculated well-differentiated airway epithelial cell (AEC) cultures derived from bovine and porcine origin with 10'000 $TCID_{50}$ and

374   monitored the viral kinetics for 96 hours. This revealed that D/CN286 replicated efficiently in both

375   bovine and porcine AEC cultures, albeit slightly higher in the swine AEC cultures **(Figure 5A, B)**. This

376   was also observed when the swine and bovine AEC cultures were infected with the cell culture-

377   adapted D/660 isolate **(Figure 5A, B)**. Interestingly, this also revealed a similar trend that had been

378   previously observed in the conventional cell lines, namely that the cell culture-adapted D/660 virus

379   replicates more efficiently compared to the D/CN286 reverse genetic clone. However, this effect

380   does not seem to correspond to any difference in cell tropism, as both viruses infected ciliated cells

381   **(Figure 5C, D)**. This observation suggests that potential discrepancies in the replication efficiency are

382   likely associated with the genetic differences between both virus stocks **(Figure 5C, D)**. Nonetheless,

383   these combined results demonstrate that we successfully established a reverse genetic clone from a

384   bovine-derived IDV isolate that efficiently replicates in different cell culture models.
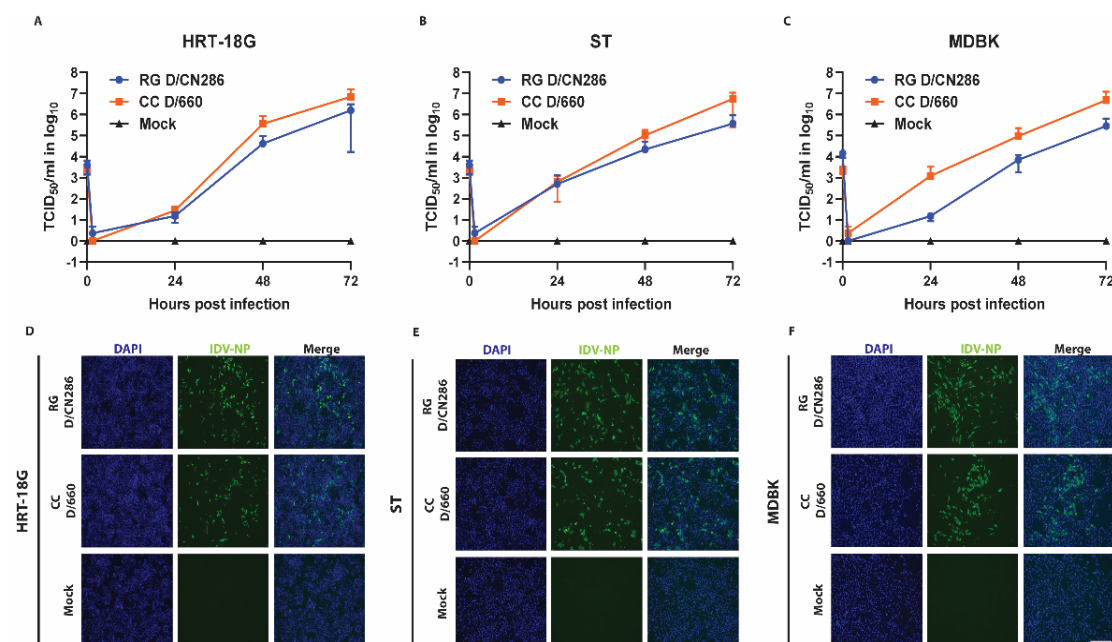

385

386   **Figure 4: Replication kinetics of IDV on conventional cell lines.** The replication kinetics of the reverse

387   genetic D/CN286 clone were compared to the cell culture-adapted D/660 isolate on cell lines of

388   human (HRT-18G, MOI: 0.01), porcine (ST, MOI: 0.01) and bovine (MDBK, MOI: 0.1) origin. Viral

389   kinetics were monitored for 72 hours with 24 hours intervals. Values depicted at 0 hours are the

390   inoculum titres. Viral titres are given as $TCID_{50}$/ml (Y-axis) of the corresponding time points (X-axis)

391   for HRT-18G **(A)**, ST **(B)** or MDBK cell lines **(C).** Data points are shown as means and SD of three

392   individual experiments performed in two technical replicates. After 72 hours of viral infection, cells

393   were formalin-fixed and immunostained with the IDV-NP polyclonal antibody (Green) and DAPI

394   (Blue). Representative microscopy images are shown of virus-infected and control culture for HRT-

395   18G **(D)**, ST **(E)** and MDBK cell lines **(F).** Images were acquired with a 10x air objective. Scale bar
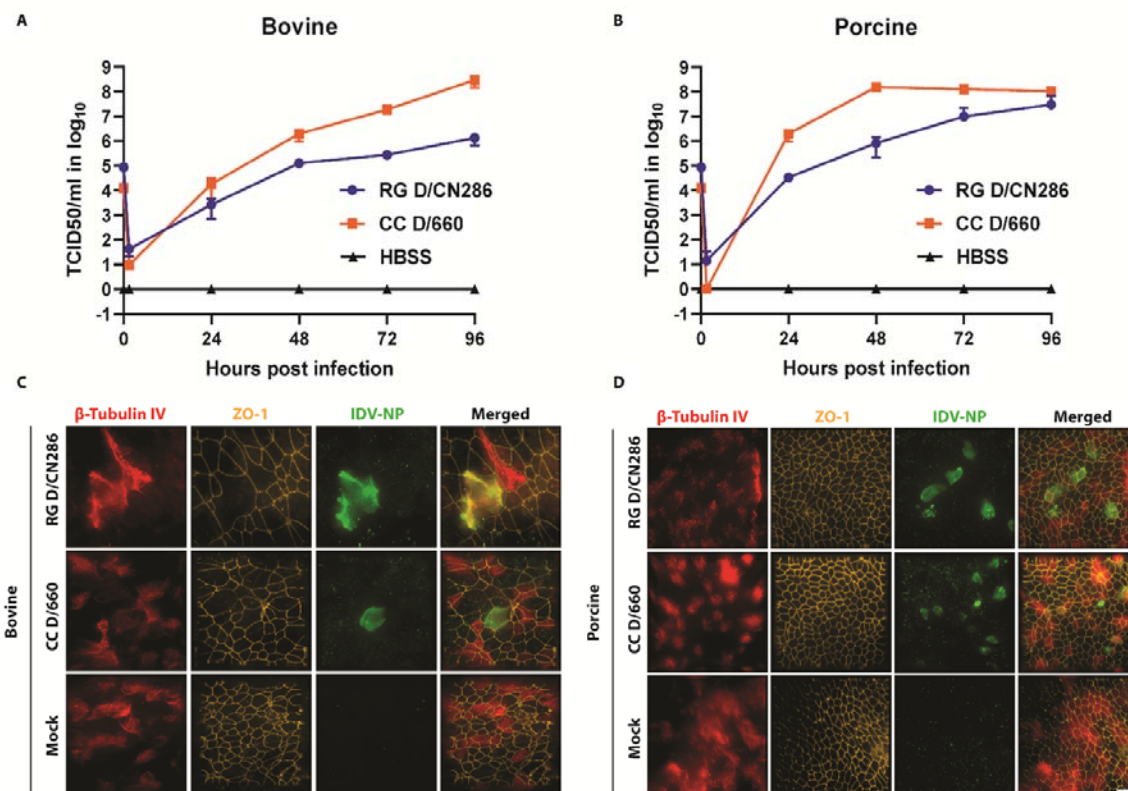
396   represents 275 µm.

397

Figure 5: Replication kinetics and determination of the cellular tropism of the rescued Influenza D virus (IDV) clone on well-differentiated airway epithelial cell (AEC) from bovine and porcine origin. AEC cultures were infected with 10.000 $TCID_{50}$ of the rescued IDV clone (RG D/CN286) or cell culture grown IDV (CC D/660). The replication kinetics were monitored for 96 hours of incubation at 37°C and 5% CO_2, whereby apical washes were collected every 24 hours and analysed by viral titration followed by formalin-fixation and preparation for immunostaining. Viral infectious titres (Y-axis) of the corresponding apical washes are shown as $TCID_{50}$/ml as indicated hours post infection (X-axis), of the infected bovine **(A)** or porcine derived AEC cultures **(B)**. Results are shown as means and SD of two technical replicates of one biological donor. Formalin-fixed AEC cultures were immunostained with antibodies visualizing cilia (β-tubulin IV, red), tight junction borders (ZO-1, orange) and virus antigen (IDV-NP, green) of bovine **(C)** and porcine **(D)** derived AEC cultures. Magnification is 60x, scale bar represents 20 μm.

411   **4. Discussion:**

412   In this study we demonstrate the establishment of a functional reverse genetic system for a
413   contemporary bovine isolate of IDV. Using 5' and 3' RACE, we demonstrate that the 11 and 12
414   terminal nucleotides on the 3' and 5' NCRs, respectively are conserved on all viral genomic segments.
415   However, using a novel minireplicon assay, we observed that the sequence length of the conserved
416   segment-specific variable regions influences the RNP driven reporter activity, irrespective of using
417   the RNP complex of the bovine D/660 or D/CN286 virus isolates. Despite the overlapping
418   functionality, viable virus could only be rescued from the pHW-2000 reverse genetic clone of
419   D/CN286, and not for D/660 isolate. The assessment of the replication competency of D/CN286 in
420   different cell culture models, including well-differentiated airway epithelial cultures from bovine and
421   porcine origin, revealed robust virus replication in all models. In combination, these results
422   demonstrate the successful establishment of a reverse genetic system from a contemporary bovine
423   IDV isolate that can be used for future identification and characterization of viral determinants
424   influencing the broad host tropism of IDV.

425   Previously, two other groups have successfully developed and established a reverse genetic
426   clone for the prototypic swine-derived isolate of IDV (D/OK) [38,46]. However, in line with our
427   results, none of the reports describe the successful establishment of an reverse genetic (RG) clone
428   for the prototypic bovine isolate D/660. Interestingly, Ishida and colleagues and our results
429   independently demonstrate that the terminal nucleotide of the 3' NCR of the viral genomic RNA
430   contains an Uracil (**Figure 1**) [38], while for the prototypic D/660 isolate the majority of genomic
431   segments are wrongly annotated. However, we demonstrate that the correction of this nucleotide
432   alone does not facilitate the successful rescue of an RG clone of D/660. This indicates that mutations
433   in the coding region of the viral genome are of influence, as we demonstrate that the 5' and 3' NCR
434   of the prototypic D/660 isolate are functional. Therefore, it would be of interest to rescue the
435   D/CN286 virus isolate with individual viral genomic segments replaced with one from the D/660. This
436   strategy might reveal which genomic segment negatively influences the rescue of the RG clone of
437   D/660.

438   In our study, we demonstrate for the first time for IDV that the length of the segment-
439   specific variable 5' and 3' NCR sequence has an influence on reporter protein expression. The 5' and
440   3' NCR sequences of the NS and HEF show the lowest reporter gene expression compared to those of
441   the other genomic segments. Interestingly, this phenomenon has also been observed for the
442   phylogenetically related Influenza C Virus, where the sequence length of the variable region in the 5'
443   NCR of the NS and PB2 segment impairs reporter gene expression [47]. Although we did not perform
444   any mutational analysis on the segment-specific variable 5' and 3' NCR in our study, it has been

445   shown previously that a single nucleotide difference can have a detrimental influence [46]. It should
446   however be noted that these results cannot be generalized to the expression levels of viral proteins,
447   as it is well documented for Influenza A virus that both the NCR and gene coding sequence
448   simultaneously can influence transcription efficiency [48,49]. Therefore, further analysis is needed to
449   determine which genomic sequence elements are of importance for IDV transcription.

450   In our study, we demonstrated that the rescued reverse genetic clone of the bovine D/CN286
451   isolate replicates in different cell culture models, including well-differentiated airway epithelial
452   cultures from bovine and porcine origin. These results demonstrate, that in addition to our in vitro
453   surrogate model of the human in vivo respiratory epithelium, IDV virus – host interactions can also be
454   studied in analogous models of porcine and bovine origin. However, in comparison to the prototypic
455   bovine D/660 isolate, our RG D/CN286 virus replicated less efficiently on the MDBK cell line and
456   airway epithelial cultures from porcine or bovine origin. This difference might be due to the fact that
457   our RG D/CN286 isolate has 64 amino acid differences compared to the prototypic D/660 isolate, of
458   which 25 are present in the HEF protein **(Supplementary Table 2)**. It is therefore plausible that these
459   differences contribute to the overall lower replication efficiency of our RG clone in our primary
460   bovine and swine AEC cultures. In addition, we previously demonstrated that the cell culture adapted
461   D/660 isolate is composed out of a pool of different genomic variants [18]. Furthermore, the D/660
462   virus has a greater genomic plasticity to adapt to different host and cellular environments compared
463   to the RG D/CN286 isolate that represents a single genomic variant [50]. Therefore, it would be of
464   interest to study the influence of the 64 amino acid differences in our reverse genetic system and
465   novel minireplicon assay, as well as in well-differentiated airway epithelial cultures from human,
466   bovine and porcine origin. These results might lead to the identification and characterization of viral
467   determinants influencing the broad host tropism of IDV.

468   In summary, here we show the establishment of a functional reverse genetic system for a
469   contemporary bovine isolate of IDV that will facilitate further characterization of IDV.

470   **Acknowledgements**

473   **Funding**

References

475

476 1. Hause, B.; Collin, E.; Liu, R.; Huang, B.; Sheng, Z.; Lu, W. Characterization of a novel influenza

477   virus strain in cattle and swine: proposal for a new genus in the Orthomyxoviridae family.

478   *MBio* **2014**, *5*, 1–10.

479 2. King, A.M.Q.; Lefkowitz, E.J.; Mushegian, A.R.; Adams, M.J.; Dutilh, B.E.; Gorbalenya, A.E.;

480   Harrach, B.; Harrison, R.L.; Junglen, S.; Knowles, N.J.; et al. *Changes to taxonomy and the*

481   *International Code of Virus Classification and Nomenclature ratified by the International*

482   *Committee on Taxonomy of Viruses (2018)*; Springer Vienna, 2018; Vol. 163; ISBN

483   0070501838471.

484 3. Hause, B.M.; Ducatez, M.; Collin, E.A.; Ran, Z.; Liu, R.; Sheng, Z.; Armien, A.; Kaplan, B.;

485   Chakravarty, S.; Hoppe, A.D.; et al. Isolation of a Novel Swine Influenza Virus from Oklahoma

486   in 2011 Which Is Distantly Related to Human Influenza C Viruses. *PLoS Pathog.* **2013**, *9*, 1–11.

487 4. Snoeck, C.J.; Oliva, J.; Pauly, M.; Losch, S.; Wildschutz, F.; Muller, C.P.; Hübschen, J.M.;

488   Ducatez, M.F. Influenza D Virus Circulation in Cattle and Swine, Luxembourg, 2012–2016.

489   *Emerg. Infect. Dis.* **2018**, *24*, 2012–2013.

490 5. Ferguson, L.; Eckard, L.; Epperson, W.B.; Long, L.P.; Smith, D.; Huston, C.; Genova, S.; Webby,

491   R.; Wan, X.F. Influenza D virus infection in Mississippi beef cattle. *Virology* **2015**, *486*, 28–34.

492 6. Horimoto, T.; Hiono, T.; Mekata, H.; Odagiri, T.; Lei, Z.; Kobayashi, T.; Norimine, J.; Inoshima,

493   Y.; Hikono, H.; Murakami, K.; et al. Nationwide distribution of bovine influenza D virus

494   infection in Japan. *PLoS One* **2016**, *11*, 1–7.

495 7. Alvarez, I.J.; Fort, M.; Pasucci, J.; Moreno, F.; Gimenez, H.; Näslund, K.; Hägglund, S.; Zohari, S.

496   Seroprevalence of influenza D virus in bulls in Argentina. *J. Vet. Diagnostic Investig.* **2020**, 1–4.

497 8. Salem, E.; Cook, E.A.J.; Lbacha, H.A.; Oliva, J.; Awoume, F.; Aplogan, G.L.; Hymann, E.C.; Muloi,

498   D.; Deem, S.L.; Alali, S.; et al. Serologic Evidence for Influenza C and D Virus among Ruminants

499   and Camelids, Africa, 1991-2015. *Emerg. Infect. Dis.* **2017**, *23*, 2015–2018.

500 9. Ducatez, M.F.; Pelletier, C.; Meyer, G. Influenza d virus in cattle, France, 2011–2014. *Emerg.*

501   *Infect. Dis.* **2015**, *21*, 368–371.

502 10. Dane, H.; Duffy, C.; Guelbenzu, M.; Hause, B.; Fee, S.; Forster, F.; McMenamy, M.J.; Lemon, K.

503   Detection of influenza D virus in bovine respiratory disease samples, UK. *Transbound. Emerg.*

504   *Dis.* **2019**, *66*, 2184–2187.

505   11.   Foni, E.; Chiapponi, C.; Baioni, L.; Zanni, I.; Merenda, M.; Rosignoli, C.; Kyriakis, C.S.; Luini,
506   M.V.; Mandola, M.L.; Nigrelli, A.D.; et al. Influenza D in Italy: towards a better understanding
507   of an emerging viral infection in swine. *Sci. Rep.* **2017**, 1–7.

508   12.   Ferguson, L.; Olivier, A.K.; Genova, S.; Epperson, W.B.; Smith, D.R.; Schneider, L.; Barton, K.;
509   McCuan, K.; Webby, R.J.; Wan, X.-F. Pathogenesis of Influenza D virus in Cattle. *J. Virol.* **2016**,
510   *90*, 5636–5642.

511   13.   Ferguson, L.; Luo, K.; Olivier, A.K.; Cunningham, F.L.; Blackmon, S.; Hanson-dorr, K.; Sun, H.;
512   Baroch, J.; Lutman, M.W.; Quade, B.; et al. Influenza D Virus Infection in Feral Swine
513   Populations , United States. *Emerg. Infect. Dis.* **2018**, *24*, 1020–1028.

514   14.   Zhai, S.; Zhang, H.; Chen, S.; Zhou, X.; Lin, T.; Liu, R.; Lv, D.; Wen, X.; Wei, W.; Wang, D.; et al.
515   Influenza D Virus in Animal Species in Guangdong province, Southern China. *Emerg. Infect.*
516   *Dis.* **2017**, *23*, 1392–1396.

517   15.   Oliva, J.; Eichenbaum, A.; Belin, J.; Gaudino, M.; Guillotin, J.; Alzieu, J.P.; Nicollet, P.; Brugidou,
518   R.; Gueneau, E.; Michel, E.; et al. Serological evidence of influenza D virus circulation among
519   cattle and small ruminants in france. *Viruses* **2019**, *11*.

520   16.   Quast, M.; Sreenivasan, C.; Sexton, G.; Nedland, H.; Singrey, A.; Fawcett, L.; Miller, G.; Lauer,
521   D.; Voss, S.; Pollock, S.; et al. Serological evidence for the presence of influenza D virus in small
522   ruminants. *Vet. Microbiol.* **2015**, *180*, 281–285.

523   17.   White, S.K.; Ma, W.; McDaniel, C.J.; Gray, G.C.; Lednicky, J.A. Serologic evidence of exposure
524   to influenza D virus among persons with occupational contact with cattle. *J. Clin. Virol.* **2016**,
525   *81*, 31–33.

526   18.   Holwerda, M.; Kelly, J.; Laloli, L.; Stürmer, I.; Portmann, J.; Stalder, H.; Dijkman, R. Determining
527   the Replication Kinetics and Cellular Tropism of Influenza D Virus on Primary Well-
528   Differentiated Human Airway Epithelial Cells. *Viruses* **2019**, *11*.

529   19.   Herfst, S.; Schrauwen, E.J.A.; Linster, M.; Chutinimitkul, S.; De, E.; Munster, V.J.; Sorrell, E.M.;
530   Bestebroer, T.M.; Burke, D.F.; Derek, J.; et al. Airborne Transmission of Influenza A/H5N1
531   Virus Between Ferrets. *Science (80-.).* **2012**, *336*, 1534–1541.

532   20.   Long, J.S.; Giotis, E.S.; Moncorgé, O.; Frise, R.; Mistry, B.; James, J.; Morisson, M.; Iqbal, M.;
533   Vignal, A.; Skinner, M.A.; et al. Species difference in ANP32A underlies influenza A virus
534   polymerase host restriction. *Nature* **2016**, *529*, 101–104.

535   21.   Moreira, É.A.; Locher, S.; Kolesnikova, L.; Bolte, H.; Aydillo, T.; García-Sastre, A.; Schwemmle,
536   M.; Zimmer, G. Synthetically derived bat influenza A-like viruses reveal a cell type- but not
537   species-specific tropism. *Proc. Natl. Acad. Sci.* **2016**, 201608821.

538   22.   Imai, M.; Watanabe, T.; Hatta, M.; Das, S.C.; Ozawa, M.; Shinya, K.; Zhong, G.; Hanson, A.;
539   Katsura, H.; Watanabe, S.; et al. Experimental adaptation of an influenza H5 HA confers
540   respiratory droplet transmission to a reassortant H5 HA/H1N1 virus in ferrets. *Nature* **2012**,
541   *486*, 420–428.

542   23.   Neumann, G. Influenza Reverse Genetics—Historical Perspective. *Cold Spring Harb. Perspect.*
543   *Med.* **2020**, a038547.

544   24.   Dou, D.; Revol, R.; Östbye, H.; Wang, H.; Daniels, R. Influenza A virus cell entry, replication,
545   virion assembly and movement. *Front. Immunol.* **2018**, *9*, 1–17.

546   25.   Payne, S. Family Orthomyxoviridae. In *Viruses: From Understanding to Investigation*; 2017; pp.
547   197–208 ISBN 9780128031094.

548   26.   Neumann, G.; Watanabe, T.; Ito, H.; Watanabe, S.; Goto, H.; Gao, P.; Hughes, M.; Perez, D.R.;
549   Donis, R.; Hoffmann, E.; et al. Generation of influenza A viruses entirely from cloned cDNAs.
550   *Proc. Natl. Acad. Sci.* **1999**, *96*, 9345–9350.

551   27.   Hoffmann, E.; Neumann, G.; Kawaoka, Y.; Hobom, G.; Webster, R.G. A DNA transfection
552   system for generation of influenza A virus from eight plasmids. *Proc. Natl. Acad. Sci.* **2000**, *97*,
553   6108–6113.

554   28.   Fodor, E.; Devenish, L.; Engelhardt, O.G.; Palese, P.; Brownlee, G.G.; García-Sastre, A. Rescue
555   of Influenza A Virus from Recombinant DNA. *J. Virol.* **1999**, *73*, 9679–9682.

556   29.   Quinlivan, M.; Zamarin, D.; García-Sastre, A.; Cullinane, A.; Chambers, T.; Palese, P.
557   Attenuation of Equine Influenza Viruses through Truncations of the NS1 Protein. *J. Virol.* **2005**,
558   *79*, 8431–8439.

559   30.   Hoffmann, E.; Mahmood, K.; Yang, C.F.; Webster, R.G.; Greenberg, H.B.; Kemble, G. Rescue of
560   influenza B virus from eight plasmids. *Proc. Natl. Acad. Sci. U. S. A.* **2002**, *99*, 11411–11416.

561   31.   Pachler, K.; Mayr, J.; Vlasak, R. A seven plasmid-based system for the rescue of influenza C
562   virus. *J. Mol. Genet. Med.* **2010**, *4*, 239–246.

563   32.   Broszeit, F.; Tzarum, N.; Zhu, X.; Nemanichvili, N.; Eggink, D.; Leenders, T.; Li, Z.; Liu, L.;
564   Wolfert, M.A.; Papanikolaou, A.; et al. N-Glycolylneuraminic Acid as a Receptor for Influenza A

565   Viruses. *Cell Rep.* **2019**, *27*, 3284-3294.e6.

566   33.   Luo, J.; Ferguson, L.; Smith, D.R.; Woolums, A.R.; Epperson, W.B.; Wan, X.F. Serological
567   evidence for high prevalence of Influenza D Viruses in Cattle, Nebraska, United States, 2003–
568   2004. *Virology* **2017**, *501*, 88–91.

569   34.   Collin, E.A.; Sheng, Z.; Lang, Y.; Ma, W.; Hause, B.M.; Li, F. Cocirculation of Two Distinct
570   Genetic and Antigenic Lineages of Proposed Influenza D Virus in Cattle. *J. Virol.* **2015**, *89*,
571   1036–1042.

572   35.   Gultom, M.; Laloli, L.; Dijkman, R. Well-Differentiated Primary Mammalian Airway Epithelial
573   Cell Cultures. In *Coronaviruses: Methods and Protocols*; Maier, H.J., Bickerton, E., Eds.;
574   Springer US: New York, NY, 2020; pp. 119–134 ISBN 978-1-0716-0900-2.

575   36.   Barger, C.J.; Branick, C.; Chee, L.; Karpf, A.R. Pan-cancer analyses reveal genomic features of
576   FOXM1 overexpression in cancer. *Cancers (Basel).* **2019**, *11*.

577   37.   Schindelin, J.; Arganda-Carreras, I.; Frise, E.; Kaynig, V.; Longair, M.; Pietzsch, T.; Preibisch, S.;
578   Rueden, C.; Saalfeld, S.; Schmid, B.; et al. Fiji: An open-source platform for biological-image
579   analysis. *Nat. Methods* 2012.

580   38.   Ishida, H.; Murakami, S.; Kamiki, H.; Matsugo, H.; Takenaka-uema, A.; Horimoto, T.
581   Establishment of a Reverse Genetics System for Influenza D Virus. *J. Virol.* **2020**, *94*, 1–13.

582   39.   Benkaroun, J.; Robertson, G.J.; Whitney, H.; Lang, A.S. Analysis of the variability in the non-
583   coding regions of influenza a viruses. *Vet. Sci.* **2018**, *5*.

584   40.   Crescenzo-Chaigne, B.; van der Werf, S. Rescue of influenza C virus from recombinant DNA. *J.*
585   *Virol.* **2007**, *81*, 11282–11289.

586   41.   Zhou, B.; Lin, X.; Wang, W.; Halpin, R.A.; Bera, J.; Stockwell, T.B.; Barr, I.G.; Wentworth, D.E.
587   Universal influenza B virus genomic amplification facilitates sequencing, diagnostics, and
588   reverse genetics. *J. Clin. Microbiol.* **2014**, *52*, 1330–1337.

589   42.   Zhou, B.; Donnelly, M.E.; Scholes, D.T.; St. George, K.; Hatta, M.; Kawaoka, Y.; Wentworth, D.E.
590   Single-Reaction Genomic Amplification Accelerates Sequencing and Vaccine Production for
591   Classical and Swine Origin Human Influenza A Viruses. *J. Virol.* **2009**, *83*, 10309–10313.

592   43.   Mänz, B.; Dornfeld, D.; Götz, V.; Zell, R.; Zimmermann, P.; Haller, O.; Kochs, G.; Schwemmle,
593   M. Pandemic Influenza A Viruses Escape from Restriction by Human MxA through Adaptive
594   Mutations in the Nucleoprotein. *PLoS Pathog.* **2013**, *9*.

595 44. Welkers, M.R.A.; Pawestri, H.A.; Fonville, J.M.; Sampurno, O.D.; Pater, M.; Holwerda, M.; Han,
596   A.X.; Russell, C.A.; Jeeninga, R.E.; Setiawaty, V.; et al. Genetic diversity and host adaptation of
597   avian H5N1 influenza viruses during human infection. *Emerg. Microbes Infect.* **2019**, *8*, 262–
598   271.

599 45. Guo, M.; Xu, Y.; Gruebele, M. Temperature dependence of protein folding kinetics in living
600   cells. *Proc. Natl. Acad. Sci. U. S. A.* **2012**, *109*, 17863–17867.

601 46. Yu, J.; Liu, R.; Zhou, B.; Chou, T.; Ghedin, E.; Sheng, Z.; Gao, R.; Zhai, S.; Wang, D.; Li, F.
602   Development and Characterization of a Reverse-Genetics System for Influenza D Virus. *J. Virol.*
603   **2019**, *93*, 1–14.

604 47. Crescenzo-Chaigne, B.; Barbezange, C.; Van Der Werf, S. Non coding extremities of the seven
605   influenza virus type C vRNA segments: Effect on transcription and replication by the type C
606   and type a polymerase complexes. *Virol. J.* **2008**, *5*, 1–11.

607 48. Maeda, Y.; Goto, H.; Horimoto, T.; Takada, A.; Kawaoka, Y. Biological significance of the U
608   residue at the -3 position of the mRNA sequences of influenza A viral segments PB1 and NA.
609   *Virus Res.* **2004**, *100*, 153–157.

610 49. Parvin, J.D.; Palese, P.; Honda, A.; Ishihama, A.; Krystal, M. Promoter analysis of influenza virus
611   RNA polymerase. *J. Virol.* **1989**, *63*, 5142–5152.

612 50. Stertz, S.; Palese, P. Genome Plasticity of Influenza Viruses. *Genome Plast. Infect. Dis.* **2014**, *2*,
613   162–177.

614